Why Modern Controllers Can Go Unstable in Practice

F. William Nesline* and Paul Zarchan†
Raytheon Company, Bedford, Massachusetts

This paper demonstrates the importance of analyzing proposed modern control system designs with classical frequency response techniques. When classical constraints such as open-loop crossover frequency are ignored, apparently robust modern control designs may go unstable for relatively innocuous plant perturbations. Modern control system designs of successively more complex plants are analyzed to reveal some problems that may occur in the design of real systems and to show how these problems can be solved so that modern control methods will be more useful to practical control system designers.

Introduction

MODERN control system design techniques are powerful tools for control system engineers. There have been many successful applications to trajectory or flight-path control. However, when high-frequency effects are considered, the direct application of modern control techniques can lead to a system that is unduly complex and unduly sensitive to plant parameter variations, noise on the control inputs, or random disturbances at the output. Each of these phenomena has been encountered by one practical designer or another,[1-4] and each has devised a design technique based on trial and error that was useful for solving that particular problem. However, no general approach has been devised that allows modern control theory to deal with these problems in a systematic way.

In this paper, examples of increasing complexity are presented, showing how modern roll autopilot designs with apparently adequate stability characteristics (good phase and gain margins) can easily go unstable. The importance of the open-loop crossover frequency is established, and its relationship to robustness is demonstrated through examples. It is shown how the weighting factors within the performance index can be adjusted to modify the open-loop gain and crossover frequency. The concepts presented in the paper can serve as aids to the designer attempting to apply modern control theory to real design problems.

Modern Control Applied to Missile Roll Control System

Air-launched missiles require active autopilot control for safe separation from modern launch aircraft because 1) the flowfield in the vicinity of the aircraft causes large torque disturbances on the missile and 2) the aircraft may be maneuvering when it releases its missile. The effects of these disturbances and initial conditions are typically sensed by rate gyros and accelerometers whose outputs are connected through autopilot control circuitry to fin actuators.

The transfer function that forms the basis of the roll autopilot design is[5]

$$\frac{\dot{\phi}}{\delta_c} = \frac{K_\delta}{\omega_{RR}} \frac{1}{1+S/\omega_{RR}} \tag{1}$$

where $\dot{\phi}$ is the roll rate, δ_c the fin deflection command, K_δ the fin effectiveness, and ω_{RR} the roll rate bandwidth. Typically the roll rate response determined from Eq. (1) is too slow and must be made faster by the autopilot. The maximum roll angle and rate must be kept within specified limits to ensure a safe and controlled launch.

The plant model of Eq. (1) must be augmented by adding another integrator to make roll angle available from the roll rate. The basic two-state plant model is shown in Fig. 1, and the scaled performance index, to be minimized, can be expressed as

$$J=\frac{1}{2}\int_0^\infty \left[\left(\frac{\delta_{CMX}}{\phi_{MX}}\right)^2\phi^2+\left(\frac{\delta_{CMX}}{\dot{\phi}_{MX}}\right)^2\dot{\phi}^2+\delta_C^2\right]dt \tag{2}$$

where ϕ_{MX} is the maximum desired value of the roll angle ϕ, $\dot{\phi}_{MX}$ the maximum desired value of the roll rate $\dot{\phi}$, and δ_{CMX} the maximum desired value of the fin command δ_C. The feedback control law is of the form

$$\delta_C = -C_1\phi - C_2\dot{\phi} \tag{3}$$

At this point it becomes necessary to solve for the control (regulator) gains. For low-order systems, this can sometimes be accomplished by solving the steady-state Riccati equations analytically. Direct integration, via digital computer, of the Riccati equations until the gains approach steady state often works for higher-order systems. However, this approach can be very expensive and time consuming, since small integration intervals and long convergence times may be required for systems with high-frequency dynamics and low damping. Fortunately, a computer program called OPTSYS (Optimum Systems Synthesis), developed by Bryson and Hall,[6] overcomes the above problems by avoiding integrating the Riccati equations. This efficient and cost-effective program is based upon the MacFarlane-Potter concept of eigenvector decomposition and incorporates the very accurate QR algorithm of Francis for determining the eigenvalues and eigenvectors of the Hamiltonian matrix.[6-9]

Using the nominal values of Table 1, OPTSYS was used to find the optimal regulator gains. The resultant gains, shown in Table 2, when incorporated into the feedback law of Eq. (3) and the plant model of Fig. 1, yielded excellent time response characteristics. The plant model can be made more realistic by the inclusion of actuator dynamics with transfer function shown in Fig. 1b, along with the resultant four-state plant. When the optimal two-state gains (assuming a perfect ac-

Presented as Paper 82-1512 at the AIAA Guidance and Control Conference, San Diego, Calif., Aug. 9-11, 1982; submitted Oct. 8, 1982, revision received June 13, 1983.

*Chief Systems Engineer, System Design Laboratory, Missile Systems Division. Associate Fellow AIAA.

†Principal Engineer, System Design Laboratory, Missile Systems Division. Member AIAA.

tuator) were used to control the four-state plant, the time responses were unstable.

The instability was eliminated by including the four-state plant model in the derivation of the controller gains and by feeding back the additional states. The resultant controller gains, derived using OPTSYS, and control law are also shown for the four-state system in Table 2.

The plant model can again be made more realistic by the inclusion of rate gyro dynamics with transfer function shown in Fig. 1c along with the resultant six-state plant. Instability was again noted in the time response when the four-state feedback gains were used with the six-state plant.

Including the six-state plant model in the derivation of the controller gains and feeding back the rate gyro states eliminated the instability. For this case the scaled performance index is

$$J=\frac{1}{2}\int_0^\infty\left[\left(\frac{\delta_{CMX}}{\phi_{MX}}\right)^2\phi_M^2+\left(\frac{\delta_{CMX}}{\dot{\phi}_{MX}}\right)^2\dot{\phi}^2+\delta_C{}^2\right]dt \qquad (4)$$

The resultant control law and gains for the six-state system are shown in Table 2.

Again the plant model can be made even more realistic by the inclusion of the effects of the first torsional mode. The flexible body transfer function of the torsional mode and the plant model are shown in Fig. 1d.

Instability was again noted in the time response when the six-state gains were used with the eight-state plant.

The instability was again eliminated by including the torsional mode dynamics in the derivation of the controller gains and by feeding back the torsional states. The resultant control law and gains for the eight-state system are shown in Table 2.

Table 1 Nominal inputs

Name	Definition	Value
ω_{RR}	Roll rate bandwidth	2 rad/s
K_δ	Fin effectiveness	9000 1/s^2
ω_A	Actuator bandwidth	100 rad/s
ζ_A	Actuator damping	0.65
ω_G	Rate gyro bandwidth	200 rad/s
ζ_G	Rate gyro damping	0.5
ω_1	Torsional mode frequency	400 rad/s
ζ_1	Torsional mode damping	0.01
K_1	Torisonal mode gain	−0.001
ϕ_{MX}	Maximum desired roll angle	10 deg
$\dot{\phi}_{MX}$	Maximum desired roll rate	300 deg/s
δ_{CMX}	Maximum desired fin deflection	30 deg

Classical Analysis of Modern Control System

The series of four examples, progressing from simple to complex plants, shows that the order of the design model must match the order of the plant just to yield a stable response to inputs. From a theoretical point of view, stability is guaranteed only when all of the parameters are known and the controller and plant order are the same.[11] From a practical point of view, since the plant model is never known precisely, this result is not acceptable. To understand the above phenomenon, classical frequency response methods[12-13] will be used to analyze the modern designs.

The concept of open-loop transfer function is the cornerstone of feedback control system analysis. Nyquist[14] showed its importance in stability and robustness analysis, and Bode[15] developed its use as a key design and synthesis element in feedback systems. The open-loop transfer function is the transfer function around the loop when the loop is broken at a point. The loop can be broken anywhere, but usually it is broken in series with some parameter whose value the designer can control to achieve a desired characteristic. While the whole open-loop transfer function is interesting, its frequency response characteristic is most illuminating to the designer. Both relative stability and robustness can be determined from analysis of the magnitude and phase of the open-loop frequency response, and even more importantly, the designer can determine from it what changes to make in the system dynamics in order to achieve his goals. The two most popular indices of relative stability are the gain and phase margins. The gain margin is the value of additional gain needed at the loop break to cause instability, assuming that the phase remains constant. The phase margin is the amount of phase lag that is needed at the loop break to cause instability, assuming that the gain remains constant. In addition to indicating relative stability, the open-loop transfer function indicates relative robustness to parameter changes. When the Bode diagram is marked with the key parameters of interest, it is sometimes possible to estimate, using simple calculations or sketches, the effect of a parameter change on system performance. For the various plants and controllers, the open-loop transfer functions with the loop broken at the error signal (δ_C in Fig. 1) are represented in Table 3.

It is apparent from these transfer functions that modern control (full state feedback) only influences the zeros of the open-loop transfer function, while the plant determines the poles.[16-17] Therefore classical modification of the open-loop transfer function by the inclusion of compensation networks is not possible with the modern approach, although work is being conducted in this area.[16] In addition, full state feedback ensures that the degree of the numerator is always one less than the degree of the denominator. Therefore, there will not necessarily be a great deal of attenuation at the higher frequencies. Table 3 also shows the open-loop gain constant to be invariant with system order. This means that only the performance index weightings can influence open-loop gain.

Table 2 Control laws and gains for high crossover frequency

Order of system	Control	Gains	
2	$-\delta_C=C_1\phi+C_2\dot{\phi}$	$C_1=3$	$C_2=0.103$
4	$-\delta_C=C_1\phi+C_2\dot{\phi}+C_3\delta+C_4\dot{\delta}$	$C_1=3$	$C_2=0.127$
		$C_3=8.81$	$C_4=0.0309$
6	$-\delta_c=C_1\phi_M+C_2\dot{\phi}+C_3\delta+C_4\dot{\delta}+C_5\dot{\phi}_M+C_6\ddot{\phi}_M$	$C_1=3$	$C_2=0.127$
		$C_3=8.84$	$C_4=0.0310$
		$C_5=0.0152$	$C_6=0.0000768$
8	$-\delta_C=C_1\phi_M+C_2\dot{\phi}+C_3\delta+C_4\dot{\delta}+C_5\dot{\phi}_M+C_6\ddot{\phi}_M+C_7\dddot{\phi}+C_8\ddddot{\phi}$	$C_1=3$	$C_2=0.223$
		$C_3=34$	$C_4=0.0705$
		$C_5=0.0129$	$C_6=0.0000894$
		$C_7=27.8$	$C_8=0.0279$

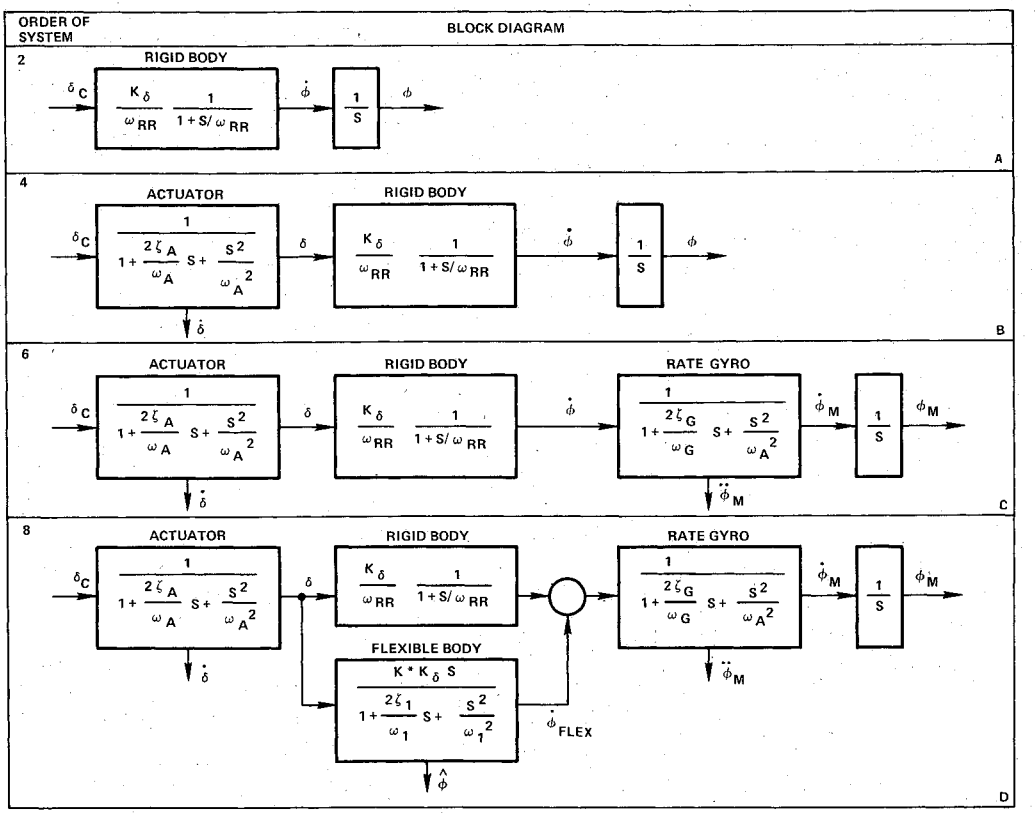

Fig. 1 System block diagram.

Typical of the Bode diagrams (complete details are in Ref. 18) is that of the matched four-state system shown in Fig. 2. At first glance this design appears to be robust (insensitive to parameter variations) because the gain margin is infinite and the phase margin is greater than 60 deg. However a closer inspection also reveals that this system has a very high crossover frequency. In fact, the crossover frequency is greater than the highest plant pole modeled, which indicates that the system is attempting to control the high-frequency dynamics. This type of high-frequency design ensures that unmodeled dynamics, occurring below crossover frequency, will cause the system to go unstable. Examination of the open-loop frequency responses of the different order systems of Table 3 shows these results to be true in general.

If a rate gyro model (making the plant sixth order) is now included with the four-state controller, the open-loop transfer function becomes

$$HG\,|_{\substack{\text{four-state ctrl}\\ \text{six-state plant}}} = \frac{13500(1+S/29.1)}{S(1+S/2)\left(1+\frac{2*0.65}{100}S+\frac{S^2}{100^2}\right)} \times \frac{\left(1+\frac{2*0.74}{173}S+\frac{S^2}{173^2}\right)}{\left(1+\frac{2*0.5}{200}S+\frac{S^2}{200^2}\right)} \tag{5}$$

Figure 3 shows that the gain and phase of the open-loop transfer function are reduced by the inclusion of the rate gyro model. Instability results (negative phase and gain margins) because the crossover frequency is too high. Updating the design model to sixth order stabilizes the system because the addition of the quadratic zero in the open-loop transfer function nearly cancels out the gyro dynamics. The high crossover frequency (327 rad/s) and low gain rolloff (20 dB/dec) ensure that this design will also be sensitive to high-

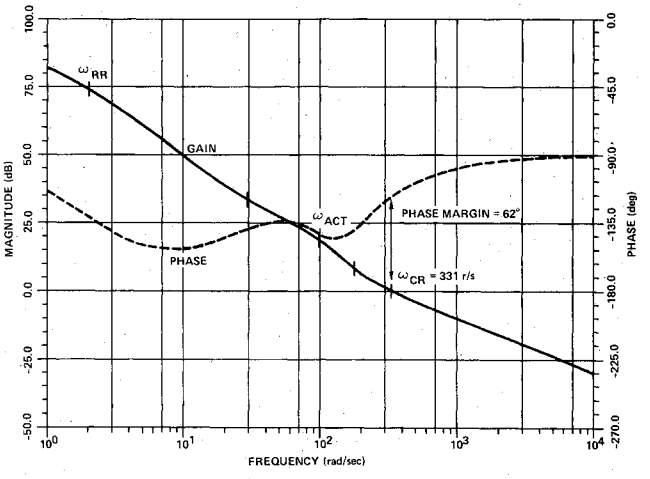

Fig. 2 Matched four-state system ($\delta_{CMX}=30$ deg) yields high crossover frequency.

frequency uncertainties in the model parameters. All model orders examined exhibited the same undesirable characteristics.

These examples, summarized in Table 3, have shown that state variable feedback modifies only the zeros of the open-loop transfer function. There is no possibility of adding extra open-loop poles by the inclusion of lag networks in the loop. For the performance index chosen, high open-loop crossover frequencies result, making the system sensitive to modeling errors. As higher-order dynamics are added to the plant, the crossover frequencies are higher than the frequencies of the added dynamics and instability results. When all the dynamics are included in the modern control design, the crossover frequency is still beyond the highest plant pole fequency, which indicates that the system is attempting to control even the high-frequency flexible body dynamics.

Use of Modern Control Theory for Practical System Design

Most of the observed problems in the previous sections were caused by the high crossover frequency. The open-loop crossover frequency can be controlled by adjusting parameters within the performance index of Eq. (2) (Ref. 19). For this example, variations in δ_{CMX} have the most profound influence on the crossover frequency as shown in Fig. 4. A classical rule of thumb is to choose the crossover frequency to be about one-third the frequency of the dynamics you do not need to control—in this case, the actuator dynamics. Then δ_{CMX} would be 0.5 deg, resulting in new control gains. These control gains reduce the open-loop gain significantly (from 13,500 to 225) as can be seen by comparing Tables 3 and 4. We can see from the Bode diagram of Fig. 5 that this open-loop transfer function has a crossover frequency of 31.7 rad/s compared to the other two-state system ($\delta_{CMX}=30$ deg) with a crossover frequency of 927 rad/s. It is apparent from the diagram that this low crossover system should be quite robust because when either actuator, rate gyro, or structural dynamics come into play, the open-loop gain is quite low.

We can demonstrate the robustness of the low crossover frequency design by combining the two-state controller with the eight-state plant. The resulting open-loop transfer function becomes

$$HG\big|_{\substack{\text{two-state ctrl}\\ \text{eight-state plant}}} = \frac{225\left(1+\dfrac{S}{14.2}\right)}{S\left(1+\dfrac{S}{2}\right)\left(1+\dfrac{2*0.65}{100}S+\dfrac{S^2}{100^2}\right)} \times \frac{1}{\left(1+1\dfrac{2*0.5}{200}S+\dfrac{S^2}{200^2}\right)\left(1+\dfrac{2*0.01}{400}S+\dfrac{S^2}{400^2}\right)} \tag{6}$$

The Bode diagram for this system is shown in Fig. 6. Even though there is a significant mismatch between controller and plant dynamics, the system is stable with adequate stability margins (phase margin = 33 deg, gain margin = 6.1 dB). The robustness is due to choosing a performance index that yields low open-loop crossover frequency. The two-state controller with the eight-state plant could give unacceptable performance at higher crossover frequencies than 31.7 rad/s because the structural damping is low enough to yield a resonant peak of 34 dB. If this is sufficient to raise the open-loop magnitude above the 0-dB line, stability problems may begin.[10,11]

If the performance index is adjusted to get low crossover frequency ($\delta_{CMX}=0.5$ deg), the control gains change. Table 4 shows how these gains influence the zeros of the open-loop transfer function. With low crossover frequency the modern control design is adding open-loop zeros to cancel out plant

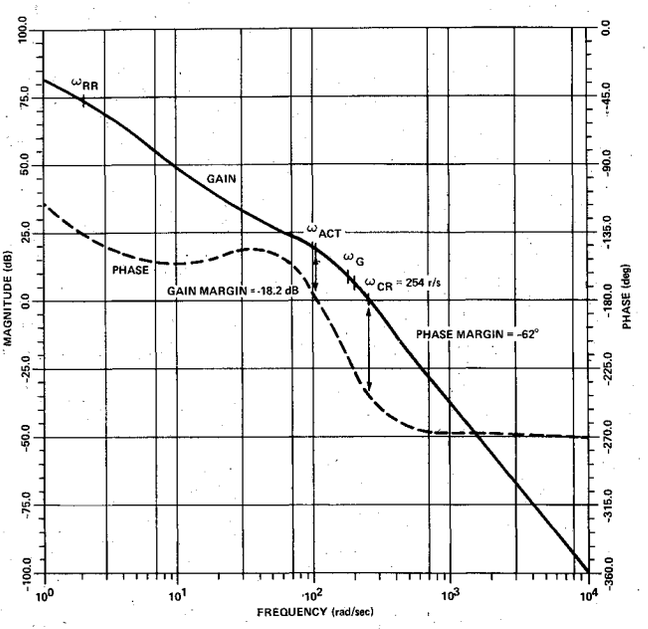

Fig. 3 Inclusion of rate gyro dynamics causes four-state controller to go unstable.

Table 3 Open-loop transfer function for high crossover frequency

Order of system	Open-loop transfer function
2	$HG=13500\ \dfrac{(1+S/29.1)}{S(1+S/2)}$
4	$HG=13500\ \dfrac{(1+S/29.1)\left(1+\dfrac{2*0.74}{173}S+\dfrac{S^2}{173^2}\right)}{S(1+S/2)\left(1+\dfrac{2*0.65}{100}S+\dfrac{S^2}{100^2}\right)}$
6	$HG=13500\ \dfrac{(1+S/29)\left(1+\dfrac{2*0.83}{160}S+\dfrac{S^2}{160^2}\right)\left(1+\dfrac{2*0.45}{216}S+\dfrac{S^2}{216^2}\right)}{S(1+S/2)\left(1+\dfrac{2*0.65}{100}S+\dfrac{S^2}{100^2}\right)\left(1+\dfrac{2*0.5}{200}S+\dfrac{S^2}{200^2}\right)}$
8	$HG=13500\ \dfrac{(1+S/18.7)(1+S/56.7)(1+S/193)\left(1+\dfrac{2*0.62}{271}S+\dfrac{S^2}{271^2}\right)\left(1+\dfrac{2*0.11}{404}S+\dfrac{S^2}{404^2}\right)}{S(1+S/2)\left(1+\dfrac{2*0.65}{100}S+\dfrac{S^2}{100^2}\right)\left(1+\dfrac{2*0.5}{200}S+\dfrac{S^2}{200^2}\right)\left(1+\dfrac{2*0.01}{400}S+\dfrac{S^2}{400^2}\right)}$

Table 4 Open-loop transfer functions for low crossover frequency

Order of system	Open-loop transfer function
2	$HG=\dfrac{225(1+S/14.2)}{S(1+S/2)}$
4	$HG=\dfrac{225(1+S/14.2)\left(1+\dfrac{2*0.66}{101}S+\dfrac{S^2}{101^2}\right)}{S(1+S/2)\left(1+\dfrac{2*0.65}{100}S+\dfrac{S^2}{100^2}\right)}$
6	$HG=\dfrac{225(1+S/14.1)\left(1+\dfrac{2*0.65}{101}S+\dfrac{S^2}{101^2}\right)\left(1+\dfrac{2*0.5}{200}S+\dfrac{S^2}{200^2}\right)}{S(1+S/2)\left(1+\dfrac{2*0.65}{100}S+\dfrac{S^2}{100^2}\right)\left(1+\dfrac{2*0.5}{200}S+\dfrac{S^2}{200^2}\right)}$
8	$HG=\dfrac{225(1+S/12.1)\left(1+\dfrac{2*0.71}{92}S+\dfrac{S^2}{92^2}\right)\left(1+\dfrac{2*0.51}{203}S+\dfrac{S^2}{203^2}\right)\left(1+\dfrac{2*0.011}{397}S+\dfrac{S^2}{397^2}\right)}{S(1+S/2)\left(+\dfrac{2*0.65}{100}S+\dfrac{S^2}{100^2}\right)\left(1+\dfrac{2*0.5}{200}S+\dfrac{S^2}{200^2}\right)\left(1+\dfrac{2*0.01}{400}S+\dfrac{S^2}{400^2}\right)}$

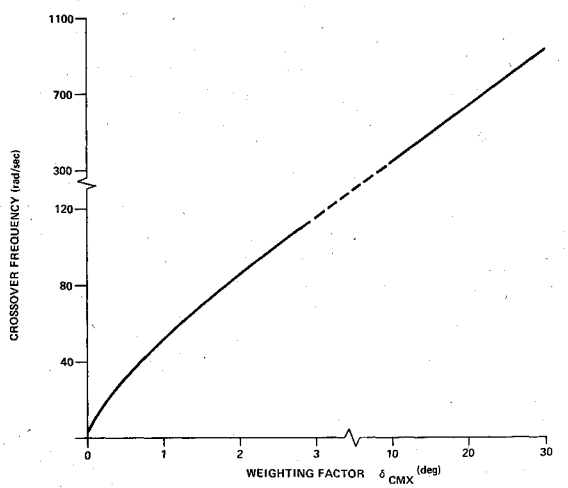

Fig. 4 Crossover frequency is proportional to weighting factor.

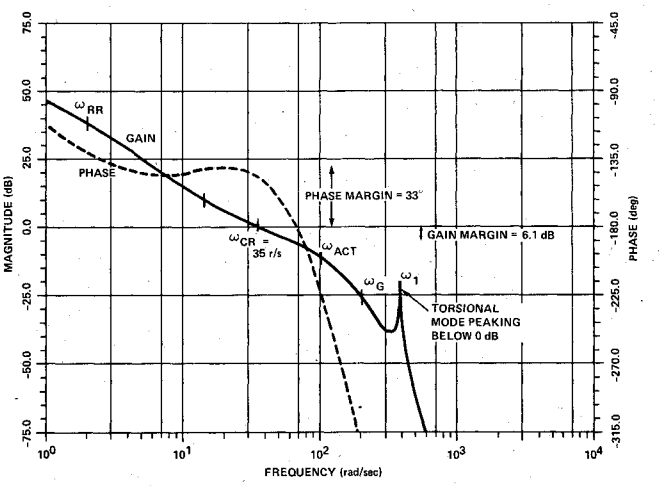

Fig. 6 Selecting low crossover frequency allows two-state controller to stabilize eight-state plant.

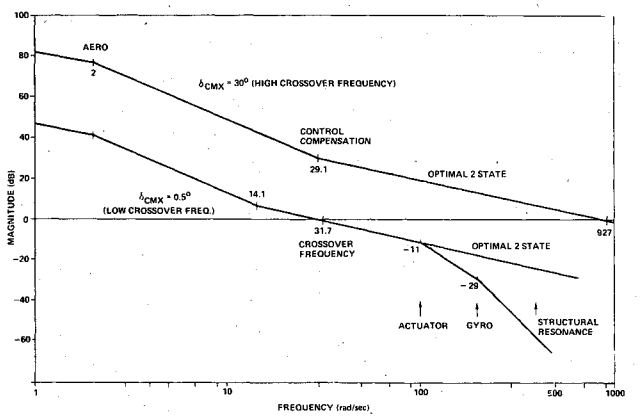

Fig. 5 Representative asymptotic Bode diagram.

poles. This type of compensation is not required for systems having many high-frequency poles if the gain is low enough at these frequencies. From a classical point of view, this type of compensation is undersirable because it complicates the controller (extra instrumentation to measure and feed back the required states) and it makes the system more sensitive to noise.

Conclusions

If a control system is designed using modern control techniques, a classical frequency response analysis must be performed to determine the crossover frequency and stability margins of the open-loop system. If the crossover frequency is too high, the system may go unstable when it is built and tested. The crossover frequency, gain, and stability margins can be modified by adjusting the weighting coefficients in the performance index until all of the required cost and sensitivity issues of the design are satisfied. This approach gives the control system engineer the flexibility required to design a practical system using modern control methods.

References

[1]Kalman, R. E., "When is a Linear Control System Optimal?" *Transactions of the ASME, Journal of Basic Engineering*, Vol. 86D, March 1964, pp. 51-60.

[2]Safonov, M. G. and Athans, M., "Gain and Phase Margin for Multiloop LQG Regulators," *IEEE Transactions on Automatic Control*, Vol. AC-22, April 1977, pp, 173-179.

[3]Anderson, B. D. O. and Moore, J. B., *Linear Optimal Control*, Prentice-Hall, Englewood Cliffs, N. J., 1971.

[4]Ashkenazi, A. and Bryson, A. E. Jr., "The Synthesis of Control Logic for Parameter-Insensitivity and Disturbance Attenuation," *Proceedings of the AIAA Guidance and Control Conference*, Aug. 1980, pp. 11-17.

[5]Nesline, F.W., Wells, B.H., and Zarchan, P., "A Combined Optimal/Classical Approach to Robust Missile Autopilot Design," *Proceedings of the AIAA Guidance and Control Conference,* Aug. 1979, pp. 265-280.

[6]Bryson, A.E. and Hall, W.E., "Optimal Control and Filter Synthesis by Eigenvector Decomposition," Stanford Univ., Stanford, Calif., SUDAAR 436, Dec. 1971.

[7]MacFarlane, A.G.J., "An Eignevctor Solution of the Linear Optimal Regulator Problem," *Journal of Electronics and Control,* Vol. 14, June 1963, pp. 643-654.

[8]Potter, J.E., "Matrix Quadratic Solution," *SIAM Journal of Applied Mathematics,* Vol. 14, No. 3, May 1966, pp. 496-501.

[9]Francis, J.G.F., "The QR Transformation," *Computer Journal,* Vol. 4, No. 3, Pt. 1, Oct. 1961, pp. 265-271; Vol. 4, Pt. II, Feb. 1962, pp. 332-345.

[10]Nesline, F.W. and Zarchan, P., "A New Look at Classical vs Modern Homing Missile Guidance," *Journal of Guidance and Control,* Vol. 4, Jan-Feb. 1981, pp. 78-85.

[11]Mahesh, J.K., Stone, C.R., Garrard, W.L., and Dunn, H.J., "Active Flutter Suppression using Linear Quadratic Gaussian Theory," *Proceedings of the AIAA Guidance and Control Conference,* Aug. 1980, pp. 265-275.

[12]Newton, G.C. Jr., Gould, L.A., and Kaiser, J.F., *Analytical Design of Linear Feedback Controls,* John Wiley & Sons, N.Y., 1957, pp. 316-343.

[13]MacFarlane, A.G.J., *Frequency-Response Methods in Control Systems,* IEEE Press, 1979, pp. 17-108.

[14]Nyquist, M., "Regeneration Theory," *Bell System Technical Journal,* Vol. II, 1932, pp. 126-247.

[15]Bode, H.W., *Network Analysis and Feedback Amplifier Design,* D. Van Nostrand Company, Inc., Toronto, 1945, pp. 188-191.

[16]Gupta, N.K., "Frequency-Shaped Cost Functionals: An Extension of Linear-Quadratic-Gaussian Design Methods, *Journal of Guidance and Control,* Vol. 3, Nov.-Dec. 1980, pp. 529-535.

[17]Sesak, J.R., Halstenberg, R.V., Chang, Y., and Davis, M.M., "Filter-Accommodated Optimal Control of Large Flexible Space Systems," *Proceedings of the AIAA Guidance and Control Conference,* Albuquerque, N.M., Aug. 1981.

[18]Nesline, F.W. and Zarchan, P., "A Classical Look at Modern Control for Missile Autopilot Design," *Proceedings of the AIAA Guidance and Control Conference,* Aug. 1982, pp. 90-104.

[19]Youla, D.C., Bongiorno, J.I. Jr., and Jabr, H.A., "Modern Wiener-Hopf Design of Optimal Controllers, Part 1: The Single-Input-Output Case," *IEEE Transactions on Automatic Control,* Vol. AC-21, Feb. 1976, pp. 3-13.